

# Capturing critical behaviour in soil moisture spatio-temporal dynamics

Antonella Di Domenico <sup>a</sup>, Giovanni Laguardia <sup>b,\*</sup>, Mauro Fiorentino <sup>a</sup>

<sup>a</sup> *Università degli Studi della Basilicata, Dipartimento di Ingegneria e Fisica dell'Ambiente, Via dell'Ateneo Lucano, 85100 Potenza, Italy*

<sup>b</sup> *European Commission – DG Joint Research Centre, Institute for Environment and Sustainability, Via E. Fermi 1, T.P.261, 21020 Ispra (VA), Italy*

Received 15 July 2005; received in revised form 31 March 2006; accepted 3 April 2006

Available online 13 June 2006

## Abstract

A physical system is subject to a phase transition process when it shows a discontinuous change of a macroscopic feature of the system under a continuous change of a system's state variable.

For certain properties of physical systems subject to phase transition it is possible to observe a scale-invariant behaviour in the point of coexistence of the phases, which in that special case is defined “critical point”.

Since the soil moisture spatial patterns in their seasonal time dynamics show the transition between spatially random to spatially connected appearances, we have investigated whether this process behaves as a critical point phenomenon. We have developed an algorithm working in analogy to the percolation theory [Bruce A, Wallace D. Critical point phenomena: the physics of the universality at large scales. In: Davis P, editor. The new physics. Cambridge: Cambridge University Press; 1989.]. The implemented methodology has been explored by applying to 365 soil moisture maps of daily data from a 507 km<sup>2</sup> natural catchment in Southern Italy. We have investigated the relation between the occupation probability in the soil moisture spatial patterns and the normalized size of the largest cluster and the behaviour of the system under changing grid scales. The critical exponents have been also calculated.

The undertaken analyses show that the process has a critical behaviour. The critical point for the examined river basin, expressed in terms of occupation probability, has a value of 0.88, which is maintained also after the coarse graining procedure.

In order to evaluate the response of the model to the choice of its parameters, we have carried out a sensitivity analysis.

© 2006 Published by Elsevier Ltd.

**Keywords:** Soil moisture; Phase transition; Percolation; Renormalization; Critical point

## 1. Introduction

Soil moisture is well recognized as a key variable in hydrology since it exerts an essential control on the water and energy balance, such as the partitioning of precipitation in infiltration and runoff and of the available energy at the land–atmosphere interface in sensible and latent fluxes.

The temporal dynamics of soil moisture can be described as the sum of two signals working at different

timescales: the first one has high frequency variability influenced by the rainfall intermittency; the second one has low frequency variability influenced by the climatic seasonality through the rainfall and potential evapotranspiration cycles. This latter is certainly that of major interest for our purposes since it controls the switching and the quantitative deviation between wet and dry seasons.

Soil water content also controls the hydraulic properties of soils. When the soil water content grows, the hydraulic conductivity also grows with a near power law, leading to the onset of the mechanisms of lateral redistribution that controls the spatial patterns of soil moisture.

As pointed out by Grayson et al. [8], in periods when precipitation continually exceeds potential evapotranspiration,

\* Corresponding author. Tel.: +39 0332 789661.

E-mail addresses: [didomenico@unibas.it](mailto:didomenico@unibas.it) (A. Di Domenico), [giovanni.laguardia@jrc.it](mailto:giovanni.laguardia@jrc.it) (G. Laguardia), [fiorentino@unibas.it](mailto:fiorentino@unibas.it) (M. Fiorentino).

the spatial patterns of soil moisture are dominated by lateral water movement by both surface and subsurface pathways; drainage lines and other areas of high topographic convergence are wetter than other parts of the catchment because of the concentration of shallow, lateral subsurface flow. When a heavy precipitation event occurs, surface runoff is generated in the wetter areas with the saturation excess mechanism. This state is dominated by the so-called non-local control.

In periods when potential evapotranspiration continually exceeds precipitation the vertical fluxes of evapotranspiration and rainfall dominate; the soil moisture patterns reflect soil and vegetation differences, taking on a more random appearance. There is no significant lateral flow and therefore no connection between a point in the catchment and its upslope area. Only in areas of high local convergence, an organization can be observed. When a heavy precipitation event occurs, surface runoff is generated in the areas where the mechanism of infiltration excess occurs. This state is dominated by the so-called local control.

As the continuous rise of soil moisture at a site (microscopic scale) controls the onset of lateral redistribution mechanisms leading the spatial patterns of soil moisture from an unorganized to an organized structure (see [8]), it is worth to look at the soil moisture processes as a system subject to phase change.

Western et al. [15] suggest that for adequately representing the soil moisture spatial variability it is necessary to catch its two essential features, namely the continuity and the connectivity. The first one represents the way the spatial correlation changes between two points and is related to the smoothness of a spatial pattern; the second one denotes the extent over which connected features (pathways having similar values) are preserved in a hydrological spatial pattern.

Geostatistical techniques provide significant tools for characterizing spatial patterns. Standard geostatistics (variogram analysis) can represent continuity but are not able to discern between patterns with or without connectivity.

Western et al. [14] show that also the variograms of indicator variables are not able to catch the connectivity: the deviations from the expected value capture differences only in continuity at different thresholds.

An alternative approach to individuate connectivity properties is to use connectivity statistics. The concept of connectivity is widely used in the context of percolation theory. The theory of percolation was first introduced years ago to describe polymerization and penetration of fluids in porous media.

Little direct use of percolation theory results has been made in the field of surface hydrology, whereas there are several applications in groundwater hydrology [1,9]. Like indicator semivariograms, connectivity statistics summarize the pattern of indicator variables. However, connectivity diagrams refer to separate points with high indicator values that are connected by any arbitrary continuous path of high values, whereas indicator variograms refer to separate points that have the same indicator value [15].

It should be noted that in order to apply connectivity statistics it is necessary to work on a binary pattern obtained by thresholding the original pattern.

The organization of soil moisture fields have been studied by cluster analysis by Rodriguez-Iturbe et al. [12]. They illustrate how soil moisture show scaling properties on its spatial clustering patterns. On the other hand, soil moisture has a crucial role as a link between hydrological and biogeophysical processes through its controlling influence on transpiration and runoff generation; consequently, the organization is also evident in the organization of vegetation of river basin [5].

This work would like to provide a contribution in the topic of soil moisture organization through concepts of the percolation theory such as cluster size, percolation probability, occupation probability, which have been dealt with in the next section.

## 2. A foreword to critical point phenomena and renormalization group concepts

Many properties of a macroscopic system are essentially determined by the connectivity of the system elements. The special behaviour of a system that emerges at the onset of macroscopic connectivity within it is known as percolation phenomenon. The theory has been extensively developed as a branch of statistical physics and has found successful applications in a wide range of problems. The principal advantage of percolation theory is that it provides universal laws that determine the geometrical and physical properties of a system. These laws are independent of local geometry or configuration of the system. In particular, many transport processes can be successfully understood by considering an idealized transport of the fluid through a conceptual medium. The flow of a fluid through a medium, which is itself in some sense disordered (or random), may be described as a so-called percolation process [1].

Percolation processes undergo a phase transition experiencing a switch from a state of local connectedness to one where the connections extend indefinitely [7]. A distinctive feature of a phase transition is a sharp change of one or more physical properties of a system under a slight change of a system state variable.

In order to illustrate the basic concepts of percolation theory that allow to characterize the connectivity, the simple model of square lattice, a reticular model, is presented.

Let the  $L \times L$  square grid consist of points representing empty and full sites connected by small capillary channels. The full sites that are connected to each other (sharing a side) represent a *cluster*. As the occupation process is random, the probability of each site being occupied is  $p = n/N$  (defined *occupation probability* or *density probability* [13]), where  $N$  is the number of the sites in the two dimensional square lattice and  $n$  is the number of them that are occupied.

In hydrological terms, the question is whether the water is able to make its way from pixel to pixel and reach the

river network. We model this problem as a two dimensional network of  $N$  points (or sites) where one site may be full (with probability  $p$ ), allowing the lateral movement, or empty (with probability  $1 - p$ ), cutting off the flow path.

It is clear that as  $p$  increases, the probability of finding larger clusters and the maximum size of the clusters also increases. In a finite lattice the lowest  $p$  value sufficiently large to ensure that at least one cluster connects the bottom and the top (or the right and the left) ends of the lattice is called *critical occupation probability*,  $p_c$ ; it is also known as the lattice site *percolation threshold*. That unique cluster is called *percolation cluster*.

Above the percolation threshold, it is possible to determine the probability  $P_\infty(p)$  that an occupied site belongs to the percolation cluster. The latter is called *percolation probability* or *cluster density* and is defined as the value of  $P_N(p) = M(L)/L^2$  when  $N$  goes to infinity, where  $M(L)$  is the number of sites that belong to the largest cluster on the  $L \times L$  lattice;  $M(L)$  is also called *mass of the largest cluster*. It has been theoretically shown and it has been confirmed experimentally and by computer simulation that  $P_\infty(p)$  has the power law behaviour  $P_\infty(p) \propto (p - p_c)^\beta$  when  $p > p_c$ , whilst it is equal to 0 for  $p < p_c$ .

The critical point  $p_c$  marks a singularity. The cluster density  $P_N(p)$  behaves singularly at this point as the size of the lattice tends to infinity: below  $p_c$  (sub-critical region) the percolation probability  $P_N(p)$  is very low, going to zero as  $L$  tends to infinity; above  $p_c$  (super-critical region) the percolation probability has a fast rise and then leaps into 1 (see Fig. 1).

The critical point behaviour denotes a special type of phase transition from a state with finite isolated clusters

to a state with at least one spanning cluster. Here, the critical point should denote the transition of soil moisture structures from an unorganized to organized appearance, i.e. the growth of variable source areas [6].

In addition to the percolation probability  $P_\infty(p)$ , another statistical property of the clusters that should be considered is the geometric extent of the cluster, also called *correlation length*,  $\xi$  (for more details see [7,13]). Similar to  $P_\infty(p)$ , the correlation length has a power law behaviour  $\xi(p) \propto |p - p_c|^{-\nu}$  when  $p < p_c$ .

For the percolation theory [3] the correlation length corresponds to the mass of the largest cluster, so  $M(p) \propto |p - p_c|^{-\nu}$  for  $p < p_c$ . The coefficients defining the power law behaviour ( $\beta$  and  $\nu$ ) are referred to as *critical exponents*. Further considerations on the *critical exponents* are presented in the following.

The percolation cluster is statistically self-similar [7], thus when looking at this cluster at a lower resolution the details will become blurred, but it will appear similar. The self-similarity leads to invariant-scale behaviour near the critical point, so the percolation cluster of the scaled lattice is qualitatively the same as the original lattice. It should be noted that the *scaling* transformation does not change the site occupation probability  $p$ , and therefore a system at  $p_c$  maintains that state even after the scale transformation.

The interconnected hillslope-channel network system possesses a profound order that remains unchanged regardless of scale, geology or climate. Like in the river basin evolution, whose planaltimetric characteristics may be identified as self-similar structures, also the soil moisture percolation cluster should be scale-invariant.

The way the scaling is carried out defines a particular process named *coarse-graining*, which is a key concept in the Renormalization Method Group. There are several kinds of *coarse-graining* procedure. The procedure, developed by Kadanoff in the 1960s, consisting of replacing group of sites by a single new site, depending on the most common value of the sites in the block, is known as the scheme of *majority rule*. Another one is the *decimation*, consisting of a deterministic or random removal of a certain number of sites from the lattice (for more details see [3]). The result of the coarse-graining is a new lattice with a new concentration of occupied sites (occupation probability)  $p_1$ , which is a function of  $p_0$  (the subscript 0 denotes the original lattice occupation probability). The technique of real-space renormalization involves the successive application of this kind of transformation (coarse-graining), obtaining the trend  $(p_n, p_{n+1})$  as in Fig. 2.

In the neighbourhood of the critical occupation probability  $p_c$ , the percolation probability  $P_\infty(p) \propto (p - p_c)^\beta$  and the correlation length  $M(p) \propto |p - p_c|^{-\nu}$  follow power laws, with  $\beta$  and  $\nu > 0$ . The coefficients  $\beta$  and  $\nu$  are called *critical exponents*, as mentioned above; they describe the “singular” behaviour of the dependent variables with respect to an increase of the independent one. Such critical exponents can point out the *universality* of the critical

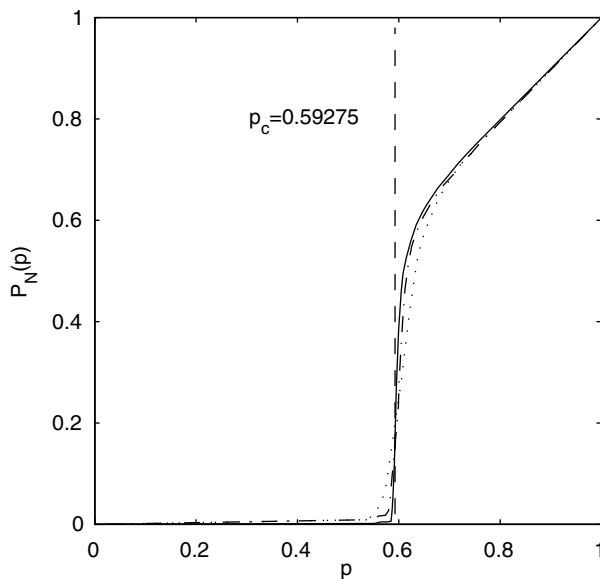


Fig. 1. Relation between the probability  $P_N(p)$  of a site belonging to the largest cluster and the occupation probability  $p$ . The solid curve is obtained for  $L = 450$ , the dash-dot curve for  $L = 200$  and the dotted curve for  $L = 50$ . The vertical line indicates  $p_c = 0.59275$  obtained by numerical simulation (see [7]).

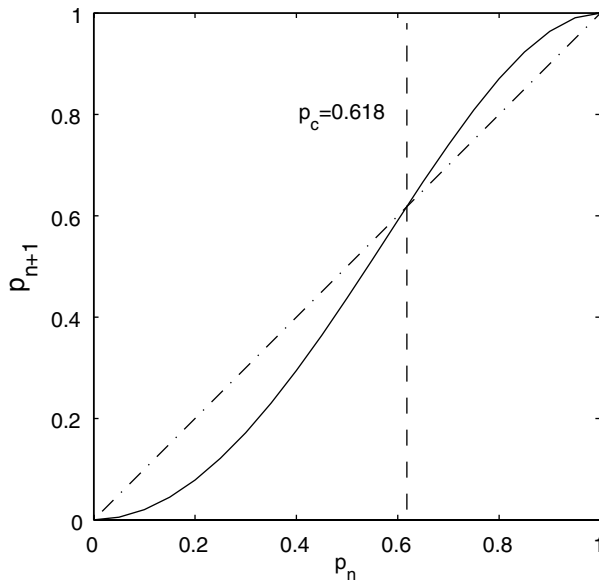


Fig. 2. Relation between the occupation probability of an  $(n + 1)$ th-order cell and the occupation probability of an  $n$ th-order cell. The critical probability for the appearance of the first percolation cluster is  $p_c = 0.618$ , that is a very good estimate obtained by renormalization method compared with  $p_c = 0.59275$  by numerical simulation.

systems, as their values are remarkably independent of the details of a certain system. The phenomenon of *universality* is the occurrence of exactly the same critical exponents in different physical systems. This involves the possibility to obtain the critical behaviour of a system from that one of other systems by means of simple transformations. This does not imply the existence of a single value for the critical exponents. Critical systems can be classified into different *universality classes*: systems in the same class have the same set of critical exponents. The critical exponents may be calculated quite accurately by renormalization method obtaining a very good estimate with brief calculation respect to long direct numerical simulation.

### 3. Model development

Soil moisture dynamics may be considered as a system that undergoes a phase transition consisting in the switch between an unorganized to an organized spatial pattern. The application of percolation theory to soil moisture fields should be in principle meaningful.

It has not been evaluated yet if this process may be considered as a critical point phenomenon. In this section, the adaptation of some notions of the percolation theory and of the renormalization group method for the application on a river basin is presented. A step-by-step example of the processing of a soil moisture map is reported in Fig. 3.

The proposed methodology works in analogy to the percolation theory though some differences exist between a percolation system and the watershed. The more evident differences are due to the definition of the system boundaries and of the fluxes exchanged with other systems.

A percolation system, for instance, consists of a rectangular lattice with two open edges; the exchange fluxes are represented by a fluid injected into a site on one edge and the fluid come out somewhere on the other edge. For our purposes, despite a much more complicated geometry, a watershed can be seen in a similar way: the incoming fluxes, the rainfall, should be subtracted of all those components not involved in the soil water content redistribution mechanisms, such as evaporation, deep percolation and surface runoff. In order to match the water balance of the system, the outcoming fluxes are represented by the subsurface runoff.

Another distinction between the percolation system and the watershed is that in the former the grid-cells are randomly filled, whereas in the latter certain properties (e.g. soils, topography) can generate preferential filling of the soils.

In the following, the model development is described.

#### 3.1. Dichotomisation

The first issue is related to the need of transforming a soil moisture map into a binary map. It has been made considering the definition of preferred states given by Grayson et al. [8]. The switching mechanism between local and non-local control is due to the non-linearity of soil hydraulic conductivity. A decrease of soil water content causes a decrease in conductivity and thus a reduction in lateral flow.

The switching value has been set on account of the  $K(\theta)$  relation (Fig. 4); thus, one assigns *zero* to pixels below the switching value and *one* to pixels above that value. The thresholding procedure has been applied to each soil moisture map once chosen the switching value (Fig. 3a and b). What is important is to point out the generality of this procedure with regards to the applicability to each map; conversely, the thresholding procedure of other analyses based on a percentile of the univariate distribution of a variable, is valid only for one map. The switching value is the first model variable which the sensitivity analysis has been carried out on.

#### 3.2. Individuation of clusters

Once the binary map has been generated, the easy up to down percolation scheme controlled by the hydraulic gradient has to be adapted to the river basin scheme. Thus, the second step consists of finding clusters of *one* pixels.

It can be reached considering the role of the orography in controlling the flow pathways; these are represented on a grid scheme by the flow direction function: two contiguous wet pixels belong to the same cluster if a flow path between them exists.

A recursive algorithm for searching *one* pixels by stepping from neighbour to neighbour in the whole map has been implemented. As each pixel has eight neighbours, it controls whether (i) at least a *one* pixel exists in the

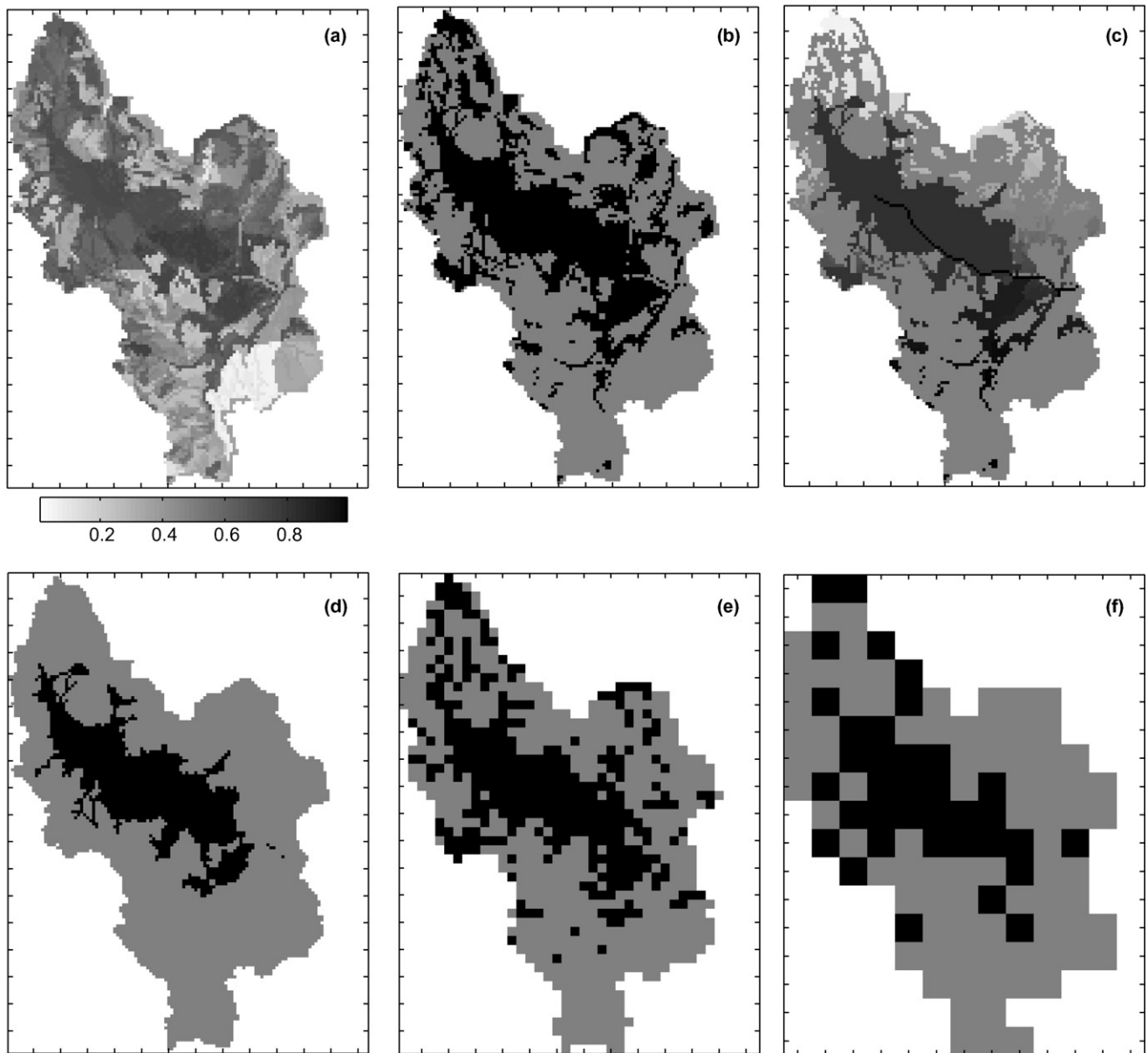


Fig. 3. The soil moisture map for June, the 10th (a) is transformed in a binary map (b) by thresholding its values; the clustering algorithm is then run producing a map detecting all the clusters (c) and then merging those being connected to the channel network and finding the largest one (d). The maps resulting after the scaling process (e,f) are also presented.

neighbourhood and (ii) it is along a possible flow path. This process labels pixels that satisfy both the previous conditions with a unique label, involving looping throughout the map. Whenever an unlabeled *one* pixel is encountered, this latter is labelled with a new label. Finally, several clusters are identified.

As discussed, until now the search of the clusters is due to geometrical and physical considerations. The clusters can be interpreted as partial contributing areas that are responsible of the runoff generation.

A further condition on the cluster aggregation has been modelled for representing the hillslope-channel system. As the time scale of the water flowing through a cluster, con-

sidered as an entity related to the sloping processes, is very large respect to the time scale of the channel flow, it is worth to consider all the clusters connected to the channel network as a whole cluster directly connected to the catchment's outlet (Fig. 3c and d). The channel network can be obtained by thresholding the flow accumulation function. Choosing the proper value for the catchment's flow accumulation is a key issue for catching the difference between slopes and channels.

The choice of the flow accumulation threshold is documented in the model application by means of comparisons with available cartography. It is the second model variable investigated by means of sensitivity analysis.



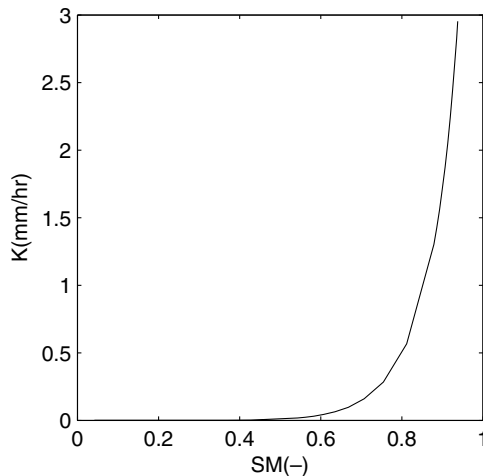


Fig. 4. Hydraulic conductivity versus water content for a medium soil.

In a catchment-like system there are no borders to connect. The assumption that a percolation cluster always exists, being that of major size, has been made; hence, *largest cluster* assumes the meaning of *percolation cluster*. As non-zero clusters exist when the occupation probability falls under its critical value, the phase change at the critical point could be not so evident.

### 3.3. Scaling transformation

The last task is related to the definition of the scaling method. We have chosen to work on three by three cell that will become a *zero* pixel in the scaled grid if there are no clusters or a *one* pixel if a cluster is found (Fig. 5). The aggregation of the clusters in each three by three cells has been carried out in the same way throughout the grid map. Finally, the occupation probability of the scaled map can be computed (Fig. 3b, e and f).

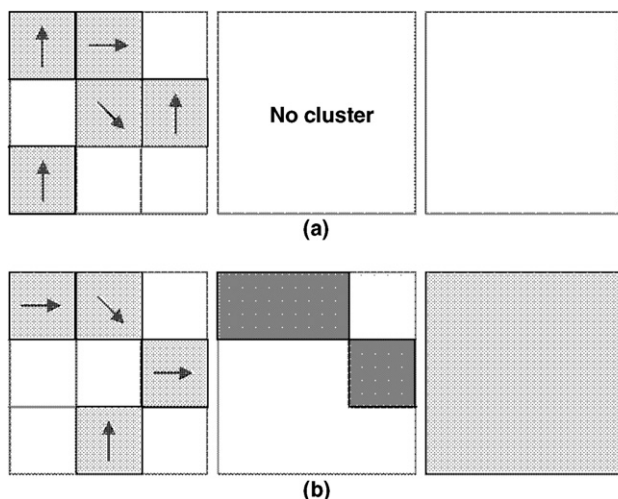


Fig. 5. Scaling transformation. *Zero* pixels are white, *one* pixels are light-grey; the arrows indicate the flow direction. (a) No cluster is found, scaled cell is *zero*; (b) a cluster is found, scaled cell is *one*.

## 4. Data collection

Soil moisture data are required for testing the methodology on a river basin. The choice of the soil moisture data source is itself a breaking issue since it is hard to match the requirements of frequency and spacing of the sampling and of accuracy of the measurement.

The availability of field data for little catchments or hillslopes is strongly limited by the small number of samples and the short time extent of the collection. As a first experiment the catchment percolation scheme has been tested on the Tarrawarra data [16], acknowledged as the best available data for catchment space/time soil moisture patterns. Unfortunately, the results obtained are quite difficult to be appreciated for the limited number of available maps. In facts, these maps allowed us to achieve only a few pairs of values  $(p, P_N(p))$ , which made it possible to barely reproduce a short piece of the curve as in Fig. 1, and more precisely the limb close to  $p = 1$ , in a region that is likely beyond the critical point. Thus, it was recognized that Tarrawarra data do not constitute a suitable sequence in order to assess the evidence of a critical point. However, it will be shown in Section 5 that the  $P_N(p)$  relationship, calculated with regard to these field data, although too scattered to show criticality, does not contrast the proposed hypothesis.

An alternative can be represented by remote sensing data. Remote sensing techniques do not allow to match the spacing requirements or to guarantee the full coverage of a catchment at a good temporal sampling. Moreover, the data are difficult to interpret due to many confounding factors, such as vegetation characteristics and soil texture.

Another option is using data obtained by simulation with a distributed hydrological model. In this way, the problems of spacing and temporal sampling can be overcome easily. On the other hand, it is needed to understand whether the model is able to represent in a reliable way the processes regulating soil moisture spatial variability.

A set of daily soil moisture maps obtained by means of the DREAM distributed hydrological model set up on the Agri catchment [11] have been made available for the present work. The DREAM model has shown good skill in reproducing the hydrologic balance as well as the probability distribution of the areas contributing to flood peaks for several river basins [10], thus soil moisture maps are expected to be quite reliable. It is useful to point out that the quality of the soil moisture maps can have only a limited effect on the results of the modelling here carried out since no strictly quantitative results are investigated.

The Agri river basin is located in the Basilicata region, southern Italy. The sub-catchment closed at the Tarangelo water level gauging station has an area of 507 km<sup>2</sup>. The elevation of this sub-catchment ranges from 500 to 1800 m a.s.l. The Agri river upstream Tarangelo drains a typical humid basin with a mean annual rainfall depth  $h = 1100$  mm and a Thornthwaite's climatic index  $I_c = (h - E_p)/E_p = 0.69$ , where  $E_p$  is the mean annual potential

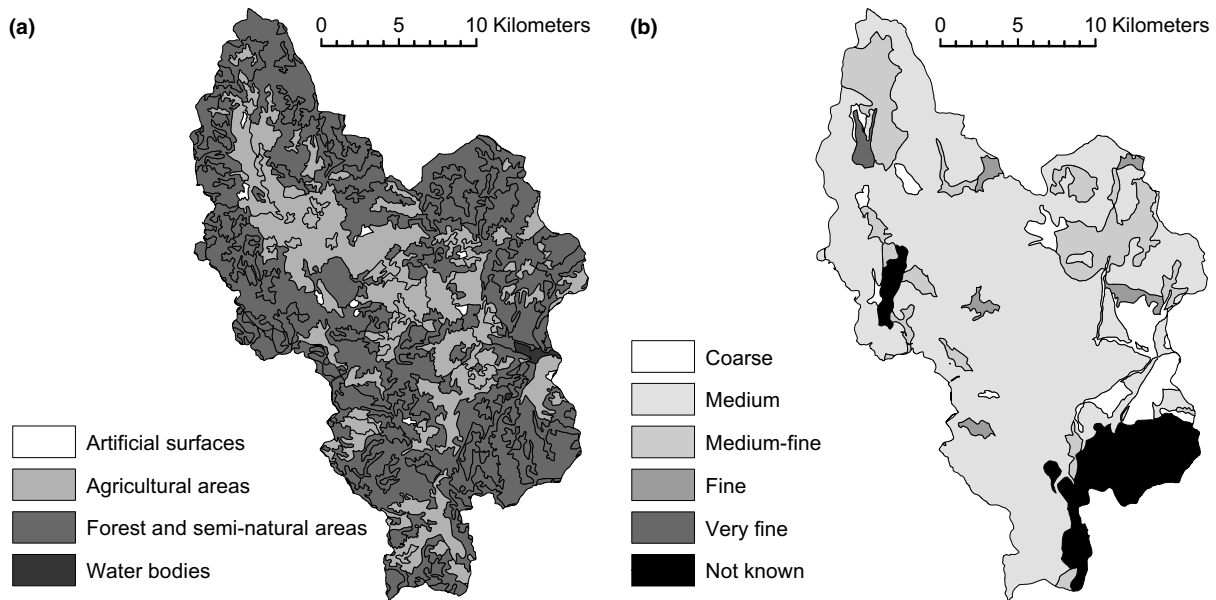


Fig. 6. Land use map (1st level of CORINE-Land Cover) (a) and soil texture map (b) for the Agri river basin at Tarangelo.

evapotranspiration. As provided by the CORINE-Land Cover Project cartography shown in Fig. 6a, the basin is mostly covered by forest and semi-natural areas (68% of the total basin surface), whereas the remaining part consists of agricultural areas (31.2%) and in a minimum part of water bodies and artificial surfaces (0.8%). Calcareous mountains and floodplains made up of gravel, sand, clay and flysch characterize the basin that comprises twelve lithological units. In Fig. 6b the soil texture map of the basin [4] is reported.

For this basin intensive data collection and modelling efforts has been carried out in the last years at the University of Basilicata. The DREAM model has been set up on a digital elevation model (DEM) with a 240 m grid resolution, which has been preserved in the soil moisture maps.

## 5. Results and discussion

The Agri catchment daily soil moisture maps at a spatial resolution of 240 m have been processed by means of the methodology described in Section 3. In Fig. 7 the average soil moisture for each map is shown. The seasonal behaviour with a wet winter and a dry summer is evident.

As a first step, we have investigated whether the spatial resolution (240 m) of the available maps can capture the separation between hillslopes and channels. At this aim, we have superimposed the river network obtained by thresholding the flow accumulation function to the slope map produced from the digital elevation model (Fig. 8a) and to a orthorectified photo map of the catchment (Fig. 8b). It is evident that the hillslopes are quite accurately delineated.

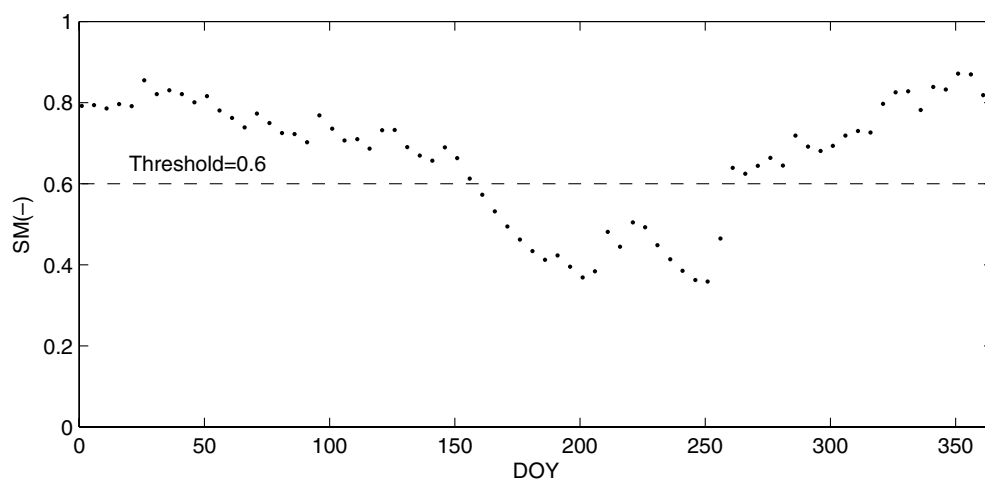


Fig. 7. Average soil moisture for Agri river basin at Tarangelo.

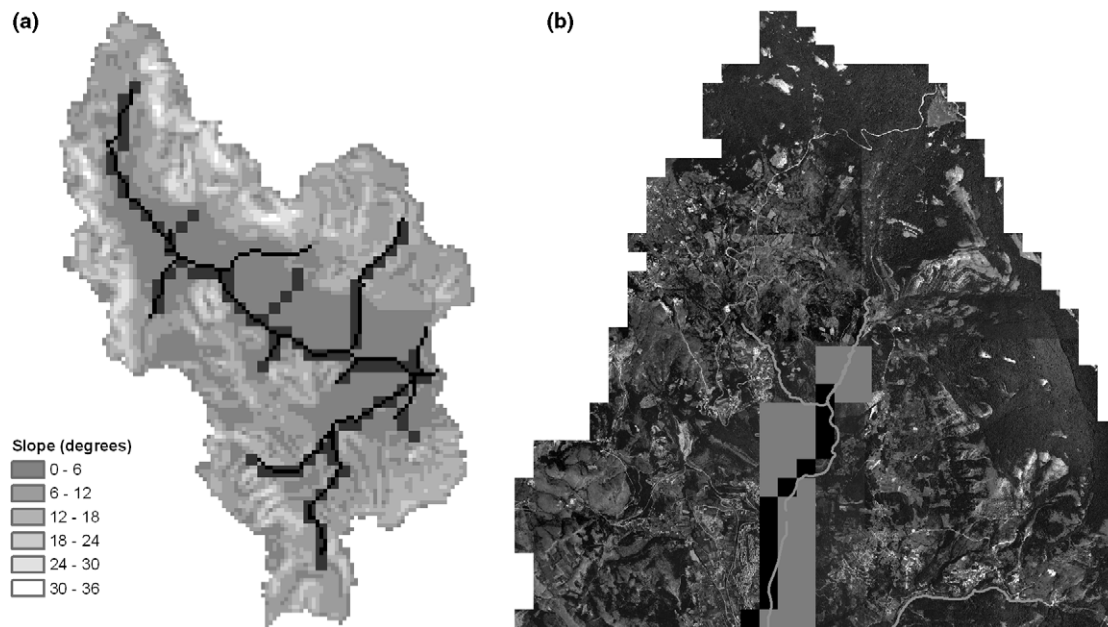


Fig. 8. (a) Slope map of the catchment. The river network obtained by the 240 m and 720 m DEMs with a flow accumulation function of  $14.4 \text{ km}^2$  are also shown. (b) Orthorectified photo map of the northern part of the catchment. The DEM based river networks are compared to the one obtained by visual inspection of the photo map.

In Fig. 8b the river network extracted by the orthorectified photo map is also shown in order to evaluate a first guess value for the flow accumulation threshold. The first guess threshold value for soil moisture has been selected by analysing its relation with soil hydraulic conductivity (Fig. 4). The effect of the flow accumulation and of the soil moisture thresholds on the results has been investigated by means of sensitivity analysis.

We have chosen  $0.6\text{--}28.8 \text{ km}^2$  thresholds as model parameters. Hence, the scaling procedure (coarse-graining) has been performed on the soil moisture maps obtained with these thresholds. The temporal evolution of  $P_N$  and  $p$  is illustrated in Fig. 9. The  $(p_0, P_N(p_0))$  scatter-plot is shown in Fig. 10.

The scaling procedure provides the scaled maps at a spatial resolution of 720 m. The occupation probability  $p_1$  for each of them has been computed. Fig. 11 shows the relation between the occupation probability before and after the scaling. Fig. 12 shows the percolation probability  $P_N(p_1)$  as a function of the occupation probability  $p_1$ .

The critical probability can be estimated as  $p_c = 0.88$  looking in Fig. 10. This value seems to be confirmed by the intersection of the  $p_0\text{--}p_1$  curve and the bisecting line (see Fig. 11). Moreover, it is almost the same after the scaling procedure (see Fig. 12).

As mentioned in Section 4, the same analysis was carried out with regard to Tarrawarra data and it was recognized that the amount of information contained in them was

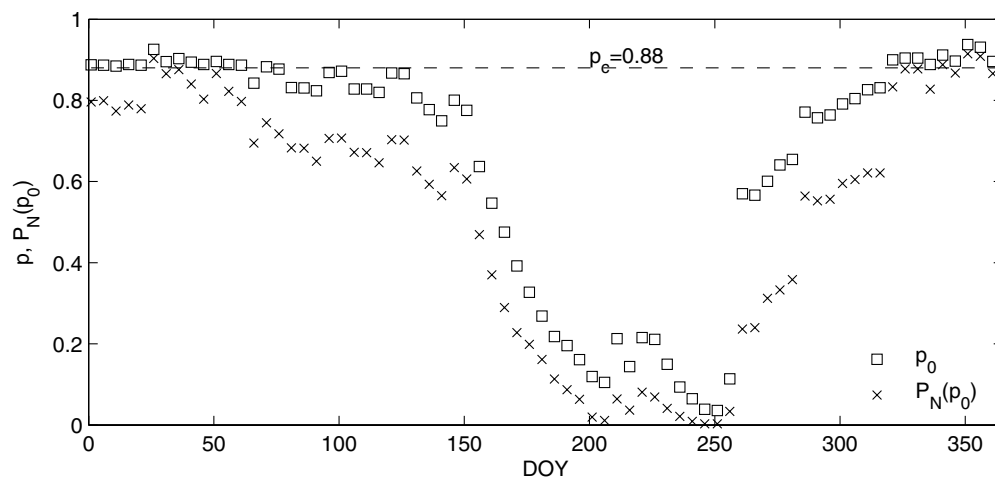


Fig. 9. Temporal evolution of occupation probability  $p$  and percolation probability  $P_N(p)$ .



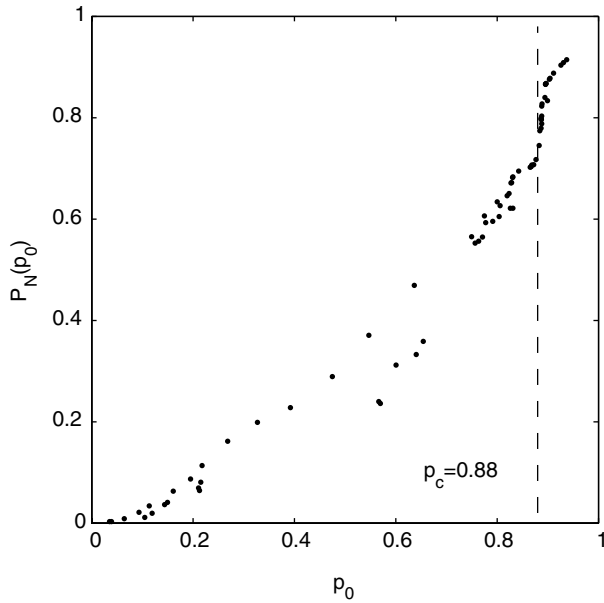


Fig. 10. Relation between the percolation probability  $P_N(p_0)$  and the occupation probability  $p_0$  for the Agri catchment soil moisture maps.

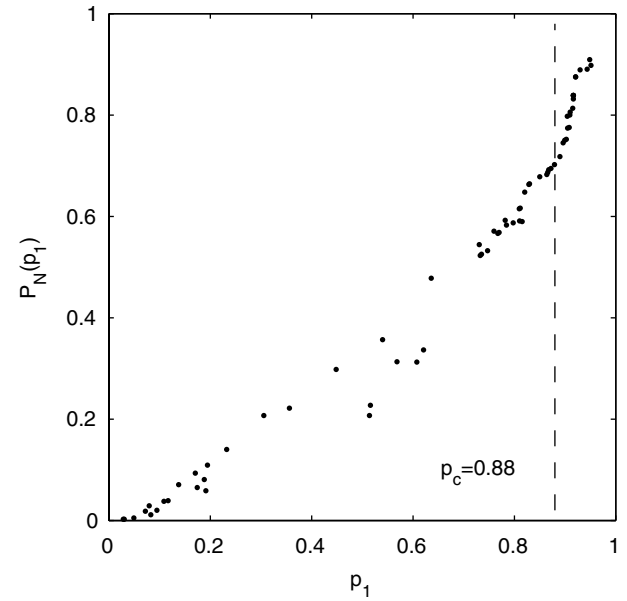


Fig. 12. Percolation probability  $P_N(p_1)$  and the occupation probability  $p_1$  after the scaling procedure.

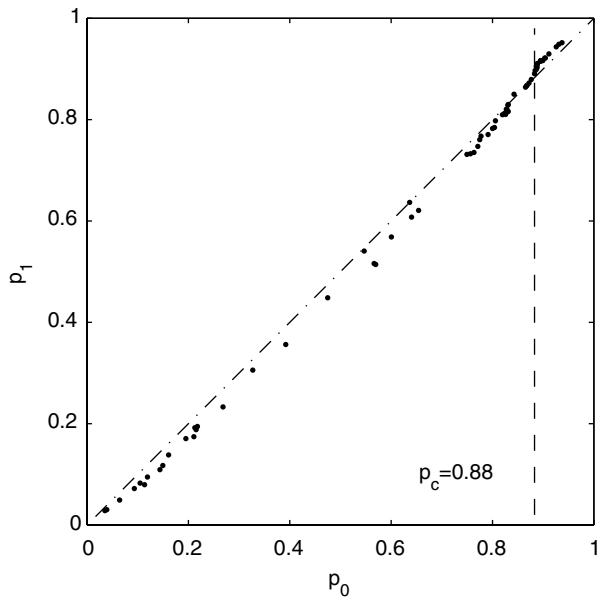


Fig. 11. Relation between the original concentration of occupied sites ( $p_0$ ) and that obtained after the scaling procedure ( $p_1$ ).

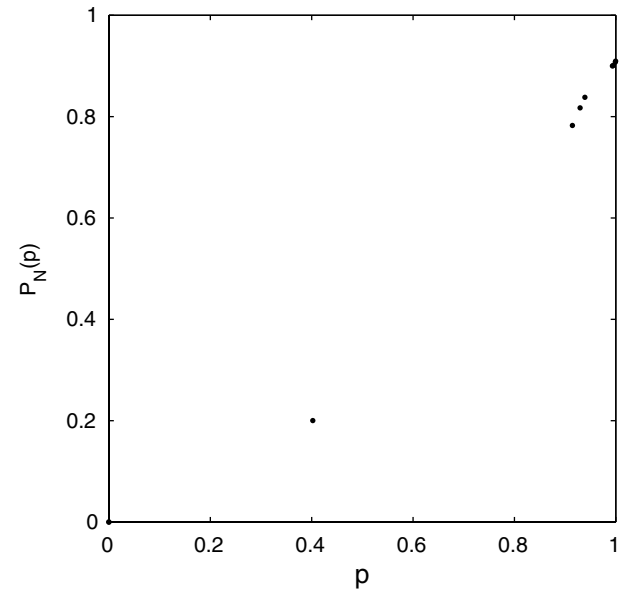


Fig. 13. Relation between the percolation probability  $P_N(p_0)$  and the occupation probability  $p_0$  for the Tarrawarra soil moisture maps.

not enough to definitely support the hypotheses proposed in this paper. This is better shown in Fig. 13 where the calculated relation between the percolation probability  $P_N(p_0)$  and the occupation probability  $p_0$  for the Tarrawarra soil moisture maps is drawn. Incidentally, to the aim of calculation, thresholds have been set to 0.30 (soil moisture) and to 7500 km<sup>2</sup> (flow accumulation). It is noteworthy that the graph, although too scattered to show criticality, does not contrast the results achieved by using simulated moisture data.

The critical probability value has been plotted also in Fig. 14 in order to evaluate the effect of the model parameters on the model behaviour.

The model has been run nine times with three different soil moisture thresholds (0.5, 0.6 and 0.7) and three different flow accumulation thresholds (14.4, 28.8 and 57.6 km<sup>2</sup>), obtaining the occupation probability ( $p_0$ ) and the associated percolation probability  $P_N(p_0)$  for all the available maps. Fig. 14 shows four of these ( $p_0, P_N(p_0)$ ) scatter-plots.

Once set the critical occupation probability, the mass of the largest clusters ( $M(L)$  for  $p < p_c$ ) and the percolation

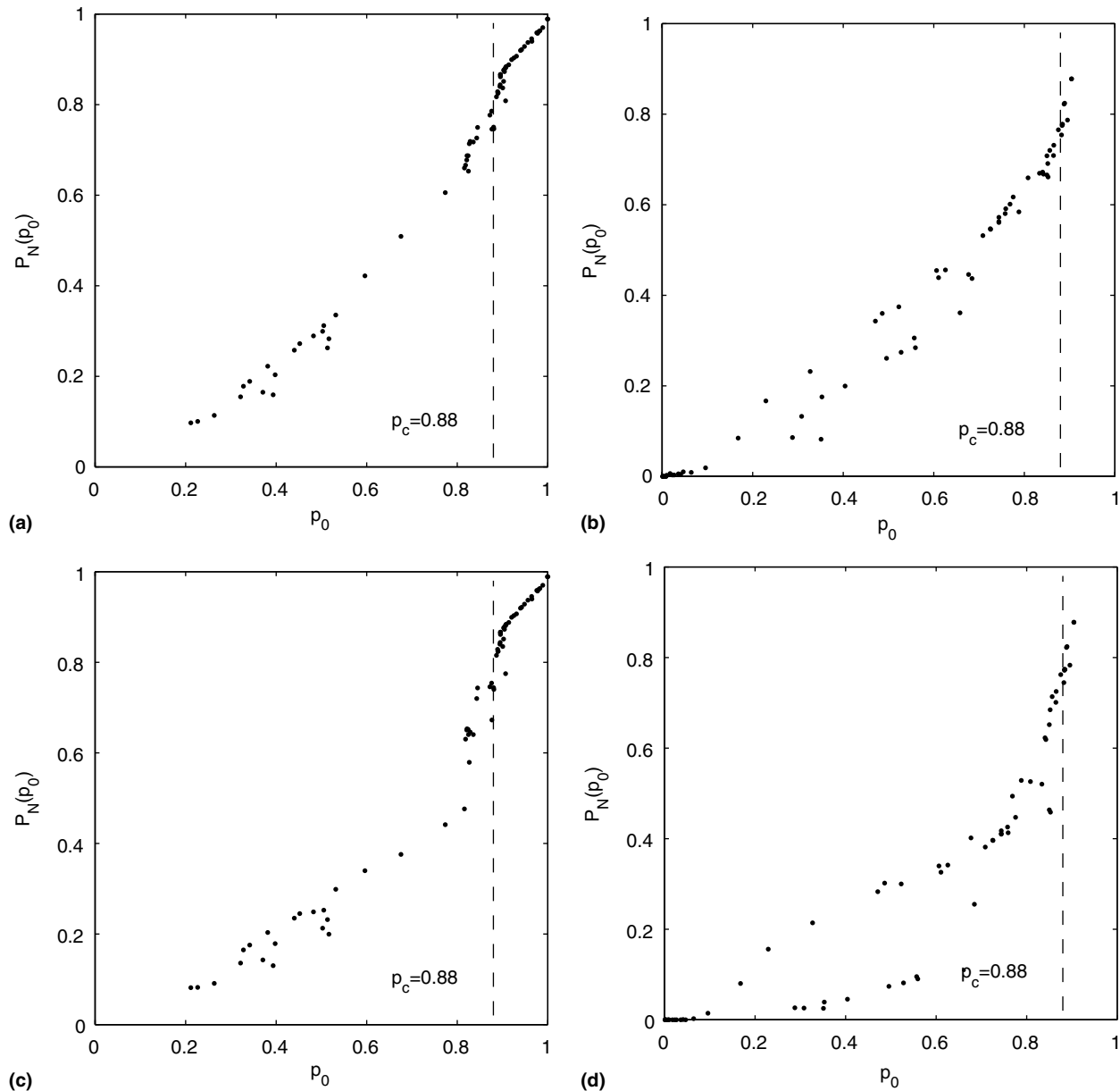


Fig. 14. Sensitivity analysis: relationship  $P_N(p_0)$  for the (a) 0.5–14.4 km<sup>2</sup>, (b) 0.7–14.4 km<sup>2</sup>, (c) 0.5–57.6 km<sup>2</sup>, (d) 0.7–57.6 km<sup>2</sup> thresholds.

probability ( $P_N(p)$  for  $p > p_c$ ) have been examined in the neighbourhood of the critical point. Figs. 15 and 16 show the relations between  $M(L)$  and  $|p - p_c|$  and between  $P_N(p)$  and  $(p - p_c)$  on a log–log scale. This proves they follow power law trends, yielding critical exponents. In the sample regarding the percolation probability (Fig. 16) the critical exponent is  $\beta = 0.13$ , whereas the critical exponent for the mass of the largest cluster (Fig. 15) is  $\nu = 0.123$ .

The analyses carried out show that the soil moisture dynamics seem to behave like a critical point phenomenon. The relations between the occupation probability and the percolation probability and between the occupation probability before and after the scaling procedure obtained by means of the methodology illustrated in Section 3 is similar to the curves shown in Figs. 1 and 2 for the percolation

model. Since in our methodology a “percolation condition” has not been defined, the value of the percolation probability is higher than zero also for  $p < p_c$  (Fig. 10); anyway, the jump of the percolation probability is almost evident as the critical occupation probability is reached.

A hysteretic behaviour is evident in the sub-critical region. It has been found that the seasonal dry to wet change (increasing  $p$ ) is carried out through the lower curve, while the wet to dry change (decreasing  $p$ ) through the upper one. Thus, the hysteresis can be associated to the persistency of organized patterns during the drying season.

In a watershed it is difficult to locate precisely the critical point because there is not a strictly sharp transition in the  $P_N(p)$  relationship. Although, the relation between the

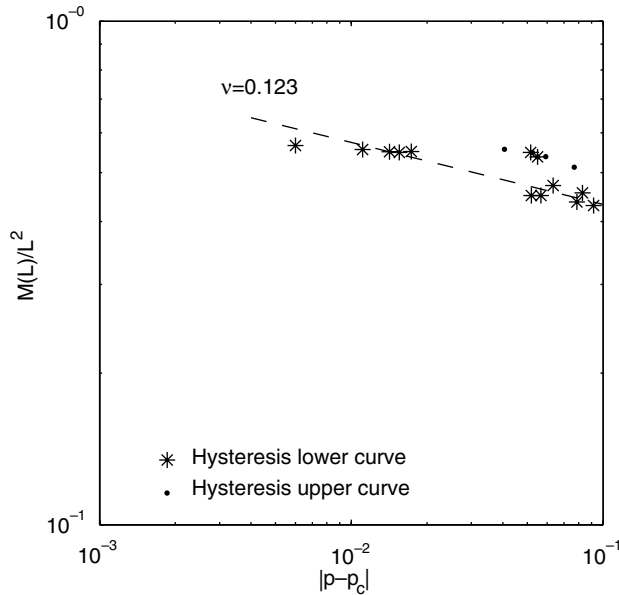


Fig. 15. Relation between the dimensionless number of sites, or mass, of the largest clusters and the reduced occupation probability plotted on a log–log scale.

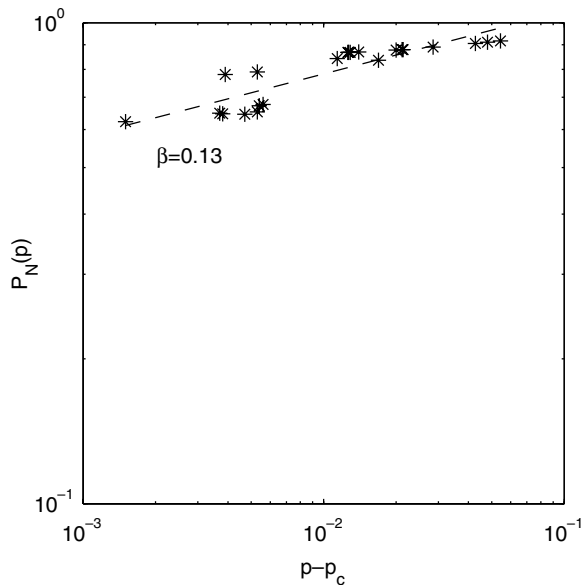


Fig. 16. Relation between the percolation probability and the reduced occupation probability plotted on a log–log scale.

occupation probability before and after the scaling should allow to better delineate the singularity in the occupation probability and especially to corroborate the previous results.

The critical point behaviour and the value of critical occupation probability determined by the  $P_N(p)$  relationship are confirmed by the typical “S” curve drawn by the points intersecting the bisecting line at  $p_c = 0.88$  (Fig. 11). Despite the perturbation of model parameters carried out in the sensitivity analysis (Fig. 14) and the application of the coarse graining procedure, the critical probability

remains almost unchanged, as well as the shape of the  $P_N(p)$  curves.

The determination of critical exponents gives way to the possibility of classifying the process in a certain universality class. From a comparison between the determined exponents ( $\nu = 0.123$  and  $\beta = 0.13$ ) and the theoretical ones, it is evident a good agreement for  $\beta$  but not for  $\nu$  with the 2D Ising model ( $\nu = 1$  and  $\beta = 1/8 = 0.125$ ; see [2]). The Ising model is one of the pillars of statistical mechanics. It tries to imitate a system in which individual elements modify their behaviour so as to conform to the behaviour of other individuals in their vicinity. It is the most influential model of a system capable of a phase transition. It was invented by W. Lenz in 1920 as a simple model of a ferromagnet, though it can be interpreted as a model of other systems too. It was solved (i.e. its critical exponents were calculated) in 2D by Onsager, but an exact solution only recently has been proposed by Zamalodchikov (see [2]). The Tsing model consists of elements or sites which are arranged in a lattice. Each site can be in one of two different states (say,  $+1/-1$ ), and each pair of neighbours interacts, in particular they have an energetic preference to achieve the same value (for more details see [3]).

The difference from the theoretical critical exponents was expected and can be explained as follows. In the Ising model the configurations are completely random, which means the mass of the largest cluster remains very low for  $p < p_c$ . Whereas the intrinsic spatial organization of the river basin, supported as well by the organized structures of the rainfall fields and also of the soil features and by the persistency of water content during the drying period (see the upper curve for  $p < p_c$  in Fig. 10), lets the mass of the largest cluster  $M(L)$  be far from zero also in dry periods.

When in the 2D Ising model the occupation probability increases, there is a rapid growth of the clusters that behave as organized spatial structures. This explains the analogies of results with the river basin soil moisture patterns for  $p > p_c$ .

## 6. Conclusions

A river basin can be considered as an open and dissipative physical system whose input energy is represented by the precipitation with its space and time variability. In analogy to other physical systems, every change of energy corresponds to a change of entropy and the principle of minimum entropy production, leading to organization, has to be respected. Those concepts, widely investigated in relation to the river network organization, have a crucial role also on the soil moisture space–time dynamics.

The spatial behaviour of soil moisture at the basin scale in its temporal dynamics has been investigated by means of the percolation theory and renormalization group method.

The soil moisture spatial patterns have shown critical point behaviour recognizable in a quick change from an unorganized to an organized structure. The existence of

the critical point has been confirmed by means of the application of the coarse graining procedure.

However, the scale invariance has not been investigated in depth because of the fast loss of spatial detail due to the coarse graining procedure and to the quite poor resolution of the initial data.

In order to assess the generality of the obtained results, we are planning to perform further research by means of the application of the model on other basins and at the hillslope scale. The choice of other soil moisture data sources will be also considered.

In the spirit of percolation theory, we have aimed to reduce the complexity of the system soil moisture of a basin to a few parameters: a percolation parameter, the occupation probability that rules the connectivity and some basic exponents, the critical exponents that describe the variations of the system close to the percolation threshold.

In this paper we have been only concerned by the willingness of discovering a critical point for the system analysed. The implication of this result, for instance its application in a study on the optimal soil moisture monitoring scale, will be addressed in forthcoming studies.

### Acknowledgements

This work is supported by MIUR in the frame of the project Cofin 2003, contract number 2003084552. We would like to thank the anonymous reviewers for their helpful comments.

### References

- [1] Berkowitz B, Balberg I. Percolation theory and its application to groundwater hydrology. *Water Resour Res* 1993;29(4):775–94.
- [2] Binney JJ, Dowrick NJ, Fisher AJ, Newmann MEJ. The theory of critical phenomena. New York: Oxford University Press; 1992.
- [3] Bruce A, Wallace D. Critical point phenomena: the physics of the universality at large scales. In: Davis P, editor. The new physics. Cambridge: Cambridge University Press; 1989.
- [4] Carriero D, Romano N, Fiorentino M. Una tecnica semplificata per la stima della distribuzione spaziale delle caratteristiche idrologiche del suolo. In: Proc 29° Convegno di Idraulica e Costruzioni Idrauliche, vol. 2. Editoriale Bios, 2004. p. 723–30.
- [5] Caylor KK, Manfreda S, Rodriguez-Iturbe I. On coupled geomorphological and ecohydrological organization of river basins. *Adv Water Resour* 2005;28(1):69–86.
- [6] Dunne T, Moore TR, Taylor CH. Recognition and prediction of runoff-producing zones in humid region. *Hydrol Sci Bull* 1975;20:305–27.
- [7] Feder J. Percolation. Fractals. New York and London: Plenum Press; 1988.
- [8] Grayson RB, Western AW, Chiew FHS. Preferred states in spatial soil moisture patterns. *Water Resour Res* 1997;33(12):2897–908.
- [9] Hristopoulos DT. Renormalization group method in subsurface hydrology: overview and applications in hydraulic conductivity upscaling. *Adv Water Resour* 2003;26(12):1279–308.
- [10] Manfreda S, Fiorentino M, Iacobellis V. Un esempio di modellistica integrata per l'analisi dei processi che controllano la frequenza delle piene fluviali. In: Proc 29° Convegno di Idraulica e Costruzioni Idrauliche, vol. 2. Editoriale Bios, 2004. p. 463–70.
- [11] Manfreda S, Fiorentino M, Iacobellis V. DREAM: a distributed model for runoff, evapotranspiration, and antecedent soil moisture simulation. *Adv Geosci* 2005;2:31–9.
- [12] Rodriguez-Iturbe I, Vogel GK, Rigon R, Entekhabi D, Castelli F, Rinaldo A. On the spatial organisation of soil moisture fields. *Geophys Res Lett* 1995;22:2757–60.
- [13] Stauffer D, Aharony A. Introduction to percolation theory. London: Taylor and Francis; 1991. 181pp.
- [14] Western AW, Blöschl G, Grayson RB. How well do indicator variograms capture the spatial connectivity of soil moisture? *Hydrol Process* 1998;12:1851–68.
- [15] Western AW, Blöschl G, Grayson RB. Toward capturing hydrologically significant connectivity in spatial patterns. *Water Resour Res* 2001;37(1):83–97.
- [16] Western AW, Grayson RB. The Tarrawarra data set: soil moisture patterns, soil characteristics and hydrological flux measurements. *Water Resour Res* 1998;34(10):2765–8.